

Phase separation in the Hubbard model

A. N. Andriotis, E. N. Economou, Qiming Li,* and C. M. Soukoulis†

Research Center of Crete and Department of Physics, University of Crete, P.O. Box 1527, 71110 Heraklion, Crete, Greece

(Received 8 October 1992)

We use the correlated-random-field approximation and a conditional coherent-potential approximation to study the ground-state phase diagram of the one-band Hubbard model. Our approach incorporates both spin and electron correlations. It has been found that for certain values of the parameters of the model, in addition to paramagnetic, ferromagnetic, antiferromagnetic, and spin-glass or spin-liquid phases found in our earlier studies, a phase-separated phase is found to be favored for $0.7 \leq n \leq 1.0$ and $U/B \geq 2$ in good agreement with results obtained in the t - J model using the technique of the $1/N$ expansion. The present approach also allows one to watch the dependence of the electron density of states on the number of electrons per site and gives a single physical picture for the occurrence of a metal-insulator transition. Implications of these results for the existence of superconducting ground state as well as comparison to other studies will be briefly discussed.

I. INTRODUCTION

The recent interest in a possible phase-separated¹ (PS) state in the Hubbard² and the related t - J models³ and the special attention that these models received in view of the strong electron-electron correlations in high- T_c superconductors and related compounds,⁴ made us undertake a systematic reexamination of the phase diagram of the Hubbard model at $T=0$, including effects due to magnetic and charge correlations. Despite strong theoretical efforts during recent years, many fundamental aspects of the solution of the Hubbard model remain yet unclear especially in the case of the two-dimensional (2D) (Refs. 5–7) and 3D systems. For these systems the problems of neglecting charge and spin correlations as well as charge and spin fluctuations from the solutions of the Hubbard model become more pronounced in the description of the $T=0$ phase diagram of the Hubbard model which remains still not clear. Recent work on the t - J model indicated that a phase-separated¹ state is a possible ground state of this model when the parameters are in a certain range. Indications for phase separation were also found by us⁸ in the Hubbard model using the correlated-random-field approximation (CRFA) and the conditional coherent-potential approximation (CPA).^{9–11}

In the present work we employ the CRFA and the conditional CPA in investigating the existence of a possible PS state of the Hubbard model. As with our previous considerations^{8,11} we use a Bethe lattice description of our system for which simple analytic expressions for the Green's functions exist.¹² A similar study for a 1D periodic Hubbard model within an unrestricted self-consistent mean-field approach¹³ has resulted in the same qualitative and quantitative results as the ones of the present approach, giving this way some additional support to our previous and recent conclusions.

II. SOLUTION OF THE HUBBARD MODEL WITHIN THE CORRELATED-RANDOM-FIELD APPROXIMATION AND THE CONDITIONAL CPA METHOD

We have employed the one-band Hubbard Hamiltonian,

$$H = \sum_{i\sigma} \epsilon_0 n_{i\sigma} + \sum_{\substack{i,j,\sigma \\ i \neq j}} V_{ij} \alpha_{i\sigma}^\dagger \alpha_{j\sigma} + U \sum_i n_{i\sigma} n_{i-\sigma} + U_1 \sum_i n_i (n_{i-1} + n_{i+1}), \quad (1)$$

where the sites (i) form a periodic lattice; σ is taken $+1$ for spin up and -1 for spin down; ϵ_0 is a constant which can be taken as zero; V_{ij} is the transfer integral which is taken to be a constant V for i, j being nearest neighbors (n.n.) and zero otherwise; U is the on-site Coulomb repulsion; and $n_{i\sigma} = \alpha_{i\sigma}^\dagger \alpha_{i\sigma}$ with $\alpha_{i\sigma}^\dagger$, $\alpha_{i\sigma}$ being the creation and annihilation operators, respectively. Finally, U_1 describes the intersite Coulomb interactions which in our case is limited only to nearest neighbors. The physical parameters of the model are the following: (i) the ratios U/V and U_1/V , (ii) the average number n of electrons per lattice site, and (iii) the type of lattice. Due to particle-hole symmetry, one obtains identical results for n and $2-n$. Thus we can restrict ourselves in the range $0 \leq n \leq 1$.

In our earlier investigation¹¹ we found solutions of the Hamiltonian of Eq. (1) (with $U_1=0$) in the CRFA. The correlated-random-field method⁹ allows us to include effects due to magnetic and charge correlations. The latter, in the simplest case, is achieved through a correlation parameter $P_{A/B}$ which denotes the probability of a lattice site being A (i.e., with the local moment up) under the condition that a given nearest-neighbor site is B (i.e.,

with the local moment down). Thus, $P_{A/B}=1$ denotes a system which exhibits perfect antiferromagnetic order, $P_{A/B}=0$ denotes perfect ferromagnetic order, while $P_{A/B}=0.5$ corresponds to a spin-glass or a spin-liquid phase. Our approximation is based on the following two steps: (i) We follow Hubbard's original suggestion and replace the cumbersome many-body U term of Eq. (1) by a random one-body term, i.e.,

$$Un_{i\sigma}n_{i-\sigma} \approx \varepsilon_{i\sigma}n_{i\sigma}, \quad (2)$$

where $\varepsilon_{i\sigma}$ are correlated random variables, the distribution of which is determined self-consistently. With this approximation, Eq. (1) is decoupled to one-spin Hamiltonians,

$$H_\sigma = \sum_i \varepsilon_{i\sigma} |i\sigma\rangle \langle i\sigma| + V \sum_{i \neq j} |i\sigma\rangle \langle j\sigma|, \quad (3)$$

where

$$\varepsilon_{i\sigma} = \varepsilon_0 + U \langle n_{i-\sigma} \rangle + U_1 \{ \langle n_{i-1} \rangle + \langle n_{i+1} \rangle \}. \quad (4)$$

(ii) We assume that the repulsive on-site interactions [U term in (1)] create local moments of fixed size μ , which can be oriented either up or down, thus we restrict the $\{\varepsilon_{i\sigma}\}$ distribution to a binary one. As a result, the solutions to Eq. (1) under the approximation of Eq. (2) can be obtained with techniques already developed for correlated-random binary alloys. It should be noted that within the present solution the size of the local moment μ as well as the parameters $P_{A/B}$ are determined self-consistently.

Under the present assumptions, we have the following binary distribution for $\{\varepsilon_{i\sigma}\}$:

$$p(\varepsilon_{i\sigma}, \varepsilon_{i-\sigma}) = x_A \delta(\varepsilon_{i\sigma} - \varepsilon_{A\sigma}) \delta(\varepsilon_{i-\sigma} - \varepsilon_{A-\sigma}) + x_B \delta(\varepsilon_{i\sigma} - \varepsilon_{B\sigma}) \delta(\varepsilon_{i-\sigma} - \varepsilon_{B-\sigma}), \quad (5)$$

where (in the absence of magnetic field) $x_A = x_B = \frac{1}{2}$ and

$$\varepsilon_{A\sigma} = \varepsilon_{B-\sigma} = \frac{1}{2}U(n - \mu), \quad (6)$$

$$\varepsilon_{A-\sigma} = \varepsilon_{B\sigma} = \frac{1}{2}U(n + \mu). \quad (7)$$

The random-field approximation of Hamiltonian (1) is associated with ground states (for the various values of n and U/V), which exhibit nonintegral moments in ordered phases as well as disordered phases which could be called "spin-glass" or "spin-liquid" states. Such states can be identified with the spin-fluid state of Anderson which has attracted interest in relation with high- T_c superconductors.

The local moment μ is determined by the self-consistency condition

$$\mu = \int_{-\infty}^{E_F} [\rho_\sigma^A(E) - \rho_{-\sigma}^A(E)] dE. \quad (8)$$

For the evaluation of μ it is obvious that we must have the electronic density of states (DOS) ρ_σ^A and $\rho_{-\sigma}^A$ which represent the average DOS for the σ and $-\sigma$ spin states, respectively, at a site where $\varepsilon_{i\sigma} = \varepsilon_{A\sigma}$ and $\varepsilon_{i-\sigma} = \varepsilon_{A-\sigma}$. The Fermi level E_F which appears in Eq. (8), is determined by the input parameter n which specifies the aver-

age number of electrons per lattice site, i.e.,

$$n = \int_{-\infty}^{E_F} [\rho_\sigma^A + \rho_{-\sigma}^A(E)] dE. \quad (9)$$

The electron DOS's $\rho_\sigma^A = \rho_{-\sigma}^B$ and $\rho_{-\sigma}^A = \rho_\sigma^B$ can be obtained from the following equations:

$$\rho_\sigma^A(E) = -\frac{1}{\pi} \lim_{s \rightarrow 0} \text{Im} \langle G_{j\sigma}(E + is) \rangle_{j=a}, \quad a = A \text{ or } B \quad (10)$$

$$G_{j\sigma}(E + is) = \left\langle j\sigma \left| \frac{1}{E + is - H_\sigma} \right| j\sigma \right\rangle, \quad (11)$$

where ε_0 in (11) and (3) has been taken for simplicity equal to $-Un/2$.

In the averaging process implied by Eq. (10) for which we employ^{9,11} the conditional CPA, off-site correlations are incorporated in H_σ through the parameter $P_{A/B}$. For $P_{A/B}=1$, we have long-range antiferromagnetism (AF) and for $P_{A/B}=0$ we have long-range ferromagnetism (F). All other intermediate cases for $P_{A/B}$ are allowed as possible solutions. The conditional CPA calculates conditionally averaged Green's functions corresponding to one or more site energies ε_i kept fixed. The other site energies $\varepsilon_j (j \neq i)$ over which the average is performed are replaced by two self-energies Σ_1 and Σ_2 periodically arranged. Σ_1 and Σ_2 are determined by the CPA condition which ensures that this replacement creates no scattering on the average in the vicinity of the site i .

Finally, the ground-state energy per lattice site is obtained from the expression (assuming that $\varepsilon_0=0$),

$$E = \frac{U}{4}(n^2 + \mu^2) + \int_{-\infty}^{E_F} [\rho_\sigma^A(E') + \rho_{-\sigma}^A(E')] E' dE', \quad (12)$$

where n and μ are the results of Eqs. (9) and (8), respectively.

It should be noted that the energy E depends on $P_{A/B}$. For given U/V and n the energetically more favorable state can be obtained by minimizing E with respect to $P_{A/B}$ [and μ ; the minimization with respect to μ is equivalent to the self-consistency, Eq. (8)].

The numerics of this model become much easier if a Bethe lattice Green's function is employed to describe the real lattice. For the Bethe lattice analytic expressions exist for the matrix elements of the Green's function in the site representation.¹² When these expressions are used, the CPA condition takes the form of two polynomial equations (with respect to the self-energies) which are solved using the iterative scheme of Newton-Ramson.

In our calculations we have used the Bethe lattice approach and calculated the ground-state energy $E = E(n, U/V, P_{A/B})$ of the system according to Eq. (12) for the given input parameters n , U/V , by $P_{A/B}$. The ground state for a given n and U/V is the one for which $E(n, U/V, P_{A/B})$ is minimum as a function of $P_{A/B}$. The ground-state energy for a given n and U/V is denoted by E_0 and the corresponding $P_{A/B}$ by $P_{A/B}^*$.

III. RESULTS AND DISCUSSION

Our original results (for $U_1=0$) for the ground state of our system in terms of U/V and n were summarized in a phase diagram shown in Fig. 1 of Refs. 8 and 11. In this phase diagram it was shown that in addition to the paramagnetic (P), ferromagnetic (F), and the antiferromagnetic (AF) phases, one new phase emerged for $U/B > 2.0$ (where the half-band-width $B=2\sqrt{K}V$, $K=Z-1$, Z being the number of nearest neighbors) namely a short-range-ordered phase characterized by $0.40 \leq P_{A/B}^* \leq 0.85$ and nonzero magnetic moments. A central part of this short-range region characterized by $P_{A/B}^* \approx 0.50$ and a nonzero magnetic moment was named the spin-glass (SG) or spin-liquid (SL) phase. A systematic analysis of our results indicated that at specific regions of the phase diagram the system favors phase separation. This was found by calculating the variation of the ground-state energy with the electron number n for given U/B . As can be seen from the present results shown in Fig. 1, for high enough U/B , the ground state of the system seems to become unstable towards phase separation. For example, for $U/B=5.0$, a two-phase system (phase one with $n=0.6$ and $P_{A/B} \approx 0.0$, i.e., ferromagnetic, and phase two with $n=1.0$ and $P_{A/B} \approx 1.0$, i.e., AF) corresponds to lower energy than the single-phase system. As U/B decreases, the phase-separation (PS) region shrinks in size. One can obtain the PS region by plotting $\Delta E = [E(n=1) - E(n)] / (1-n)$ versus n . If ΔE versus n has a minimum, this clearly shows that the PS region has lower energy than the single-phase system. This particular procedure was used to obtain the phase diagram shown in Fig. 2. Note that for large values of U/B

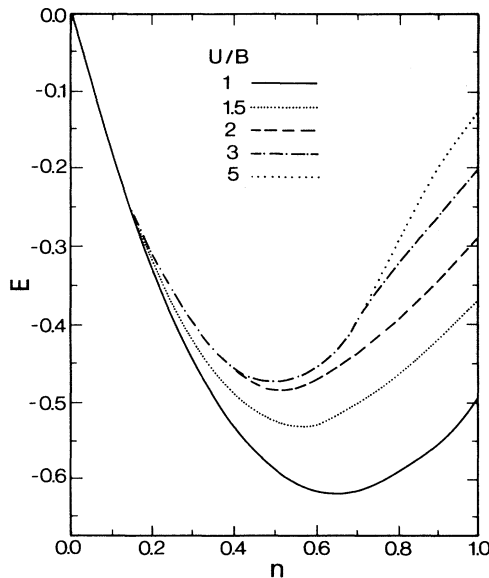


FIG. 1. The ground-state energy E (in units of $B/2$) as a function of the electron number n for different value for U/B of the 3D [Bethe lattice with connectivity (Ref. 12) $K=5$] Hubbard model. Notice that for $U/B=5$, the E vs n is clearly concave and therefore the system becomes unstable towards phase separation.

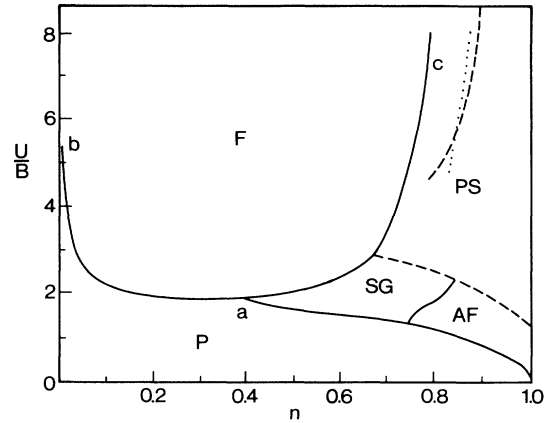


FIG. 2. The phase diagram of a 3D Hubbard system described by a Bethe lattice of connectivity $K=5$ as obtained within the conditional CPA. In addition to the paramagnetic (P), ferromagnetic (F), antiferromagnetic (AF), and spin-glass or spin-liquid (SG) phases, a phase-separated (PS) state appears to be favored for $0.7 \leq n < 1.0$ and $U/B \geq 2$. The dashed line is Nagaoka's result (Ref. 15) for the instability of the ferromagnetic state and the dotted line is the result of the approximate theory (see the Appendix) for the instability of the ferromagnetic state towards phase separation.

(≥ 1.5) and n close to 1, the PS region has lower energy. Of course at $n=1$, for all values of U/B , the system is in the AF phase. Once $n \neq 1$, the PS region sets in. In our numerical studies it was difficult to observe the PS region for $U/B \leq 1$. We, therefore, expect that the single-phase AF region has lower energy for $U/B \leq 1$. These results were obtained for a Bethe lattice of connectivity $K=5$.

It must be pointed out that our results for a phase-separated region in the Hubbard model are consistent with similar results⁷ in the t - J model obtained through

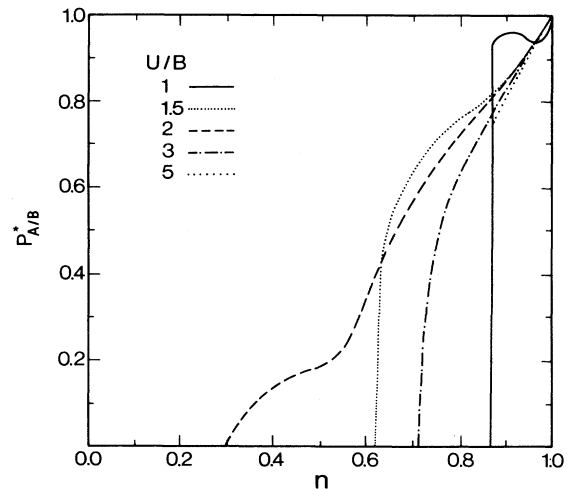


FIG. 3. Variations of the short-range parameter $P = P_{A/B}^*$ (which minimizes the ground-state energy for given n and U/B) as a function of n for a Bethe lattice of connectivity $K=5$, for different values of U/B .

the quite different approximate technique of the $1/N$ expansion. An approximate method based on the results for the ground-state energy of the F and AF states shows again that there is a region where the phase-separated state has lower energy than both the F and the AF states (see the Appendix).

In Fig. 3, we present the calculated values of $P_{A/B}^*$ as a function of n for different values of U/B . According to

Fig. 3, the off-site correlations exhibit a more or less abrupt change at values of n , which depend on U/B , where the system changes from AF or PS to ferromagnetic or paramagnetic. As U/B increases, we observe a more gradual transition to the ferromagnetic state and at lower values of n . A further increase of U/B makes the transition less gradual and at higher values of n . For very small values of $1-n$ the decrease of $P_{A/B}^*$ from its

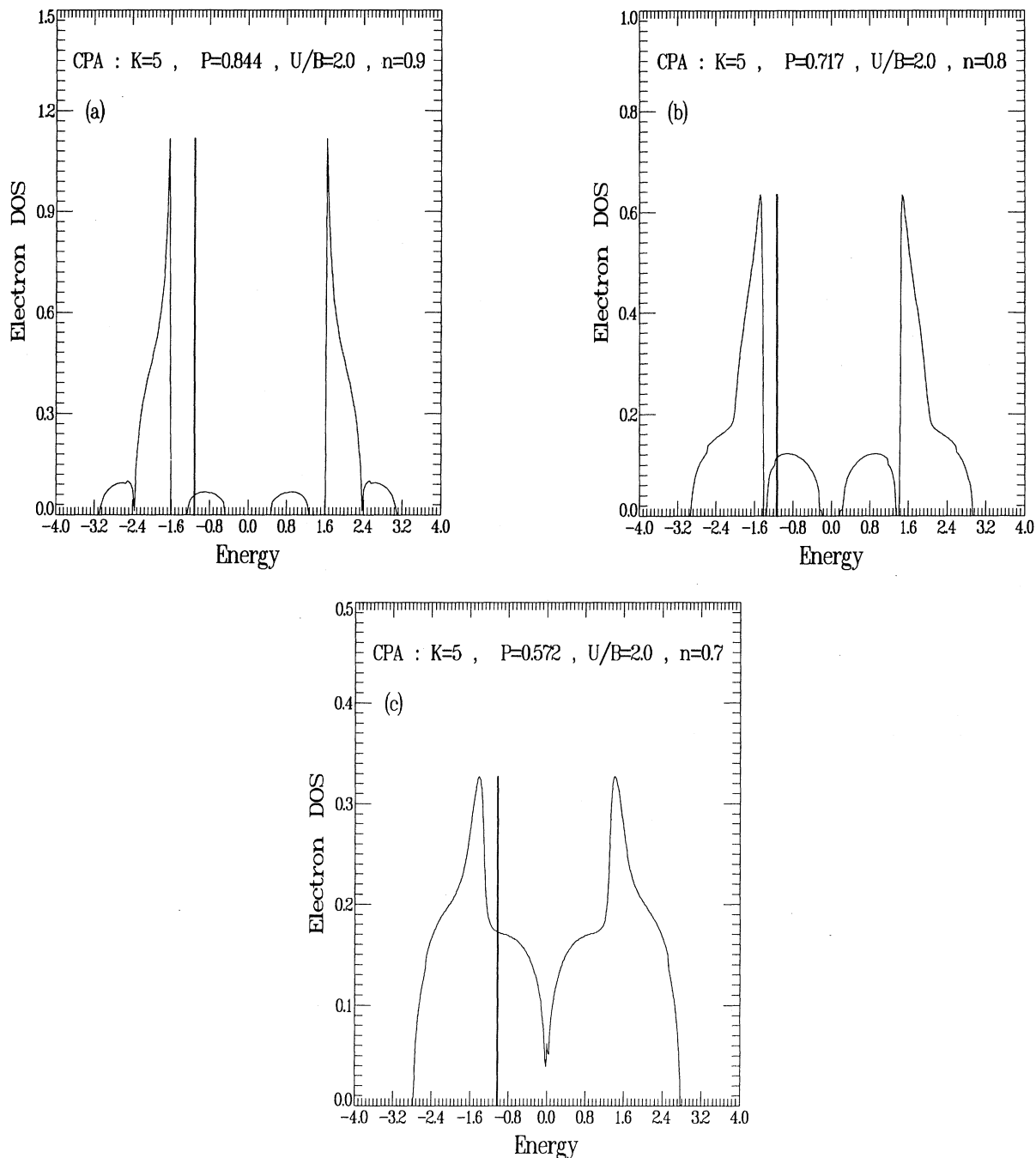


FIG. 4. Calculated electron density of states within the CRFA and a conditional CPA for a Hubbard model described by $U/B=2.0$, $K=5$ and (a) $n=0.9$ and $P_{A/B}^*=0.844$; (b) $n=0.8$ and $P_{A/B}^*=0.717$, and (c) $n=0.7$ and $P_{A/B}^*=0.572$. The position of the Fermi level is indicated by the thick vertical line.

value at $n = 1$ ($P_{A/B}^* = 1$) is associated with the reversal of some isolated local moments giving rise to a low concentration of small ferromagnetic clusters in an otherwise AF medium. This reversal of a few local moments creates two very narrow symmetric impurity subbands in the gap between the main Hubbard subbands (see also Ref. 14). This is shown in Figs. 4(a)–4(c) where we present the calculated electron density of states (DOS) for three systems that are described by the same parameter $U/B = 2.0$ but with different number of electrons n . All calculations refer to Bethe lattices with connectivity $K = 5$ and have been performed at the optimum value of the correlation parameter $P_{A/B}^*$ obtained from the results shown in Fig. 3. In particular, Fig. 4(a) refers to a system with $n = 0.9$ (for which $P_{A/B}^* = 0.844$), Fig. 4(b) to a system with $n = 0.8$ (for which $P_{A/B}^* = 0.717$), and Fig. 4(c) to a system with $n = 0.7$ (for which $P_{A/B}^* = 0.572$). Figures 4(a)–4(c) indicate clearly the creation of the impurity subbands and their systematic trends. Thus, it is observed that as $P_{A/B}^*$ gets smaller, the states in the subbands increase, while the simultaneous decrease of n results in a decrease in the distance between the locations of the bands. As a result, the subbands get closer to the main bands [Fig. 4(b)] and finally merge in two overlapping main bands [Fig. 4(c)]. It is interesting to make notice of the location of the Fermi energy in Figs. 4(a)–4(c). In Fig. 4(a) the Fermi energy is found to be at the bottom of the lower subband and remains in this subband as n gets smaller [Fig. 4(b)]. In the case where the lower subband starts overlapping with the lower main band it is still clear that the Fermi energy remains in the lower subband (as it is observed that the Fermi energy is to the right of the main peak of the lower band, i.e., to the right of the lower main band). In the case of $n = 0.9$ [Fig. 4(a)], we have found that an increase of 0.015 in the value of $P_{A/B}^*$ shifts the Fermi energy to the top of the lower main band and the system appears to be an insulator rather than a metal. In the case of $n = 0.8$ similar changes in $P_{A/B}^*$ do not change appreciably the location of the Fermi level which remains in the lower subband. From these observations we can conclude that the metal-insulator transition happens within the prescribed accuracy for $n \approx 0.9$ when $U/B = 2.0$.

The behavior of the local moment μ (without quantum fluctuations) as a function of n for different values of U/B is shown in Fig. 5. Here we observe that $\mu(n)$ follows the $\mu = n$ line rather closely for $U/B \geq 3$, departing from it for small n (where the system becomes paramagnetic) and to a small but increasing extent as n exceeds 0.6 and approaches unity. For small values of U/B ($U/B < 1.5$), $\mu = 0$ for small values of n where the system is in its paramagnetic phase, and, beyond a certain value of n , increases rather abruptly.

We have also calculated the coupling constant J of an equivalent Ising model as a function of n for different values of U/B . This constant has been calculated at $T = 0$ according to the formula $J = (\partial E / \partial P_{A/B})_T$. There are strong fluctuations in the calculated values of J . Nevertheless, the main features of the coupling constant J is the appearance of significant values of J for $n \geq 0.85$ for all values of U/B . As can be seen from Fig. 3, in this re-

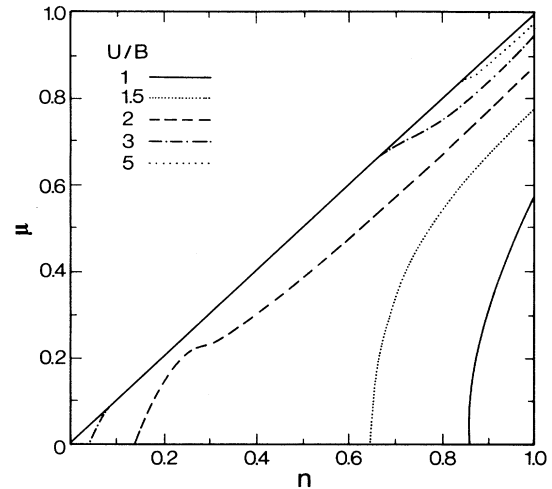


FIG. 5. Variation of the magnetic moment μ per lattice site as a function of the electron number n for a Bethe lattice of connectivity $K = 5$, for different values of U/B .

gion ($n \geq 0.85$) the ground state exhibits short-range correlations of nearly AF order.

It must be pointed out that our method, although quite sophisticated, omits quantum fluctuations which may drive the system to different ground states. This was shown by recent theoretical and numerical investigations^{16–19} on the exact spin-spin correlations of the 1D Hubbard and the t - J models which indicated that for such systems the ground state is short-range AF. The picture that emerges from these exact 1D considerations indicates the effect of neglecting quantum fluctuations and the limitations of the mean-field approaches which adopt such an approximation. However in systems of higher dimensionality (2D and 3D as in the present case), one might expect the effect of quantum fluctuations not to be strong enough (as in the 1D case) to overcome the short-range order and therefore this may possibly allow the system to attain a phase-separated state, although the existence of other configurations of even lower energy cannot be ruled out by the present calculations.

IV. CONCLUSION

We undertook a systematic analysis of the magnetic phase diagram of the Hubbard model employing the CRFA and a conditional CPA within a Bethe-lattice description of the 3D system. The analysis of the $E - n$ curves has revealed that in addition to the previously found phases (paramagnetic, ferromagnetic, antiferromagnetic, and spin glass or spin liquid), a new phase, namely, the phase-separated one, is found to be favored for $0.7 \leq n \leq 1.0$ and $U/B \geq 2$ in qualitative agreement with the results of other mean-field theories.¹

The relevance of a PS state to real materials has been questioned on the basis of the following argument: If atomic diffusion is absent, the PS state implies macroscopic net charge accumulation which in view of the long-range nature of the Coulomb forces is obviously en-

ergetically unfavorable; thus, according to this argument, the PS state, if it exists at all, is a peculiarity of the Hubbard model and has no relevance to the real world. However, if atomic diffusion is present (and there is evidence for oxygen diffusion in high- T_c superconductors), the net electronic charge accumulation or depletion can be canceled at least locally by the charge created by the diffusion of oxygen ions; consequently, the survival of a microphase-separated state, consisting of microscopic or mesoscopic domains of each (charge neutralized) phase mixed together, is possible.

Within the present approach we were also able to watch the effect of the short-range electron correlations on the electron DOS of the system and give the physical reasoning for the occurrence of a metal-insulator transition. In particular, we demonstrated the creation of two symmetric subbands between the two (symmetric) main bands. The Fermi level was found to be located at the bottom of the lower subband and at specific values of the parameters of the system to be shifted to the top of the lower subband giving rise to a metal-insulator transition.

ACKNOWLEDGMENTS

This work was partially supported by an EEC research grant (Esprit-3041), the Commission of the European Communities through grant SCC* CT90-0020, and the NATO travel grant RG769/87. The work of C.M.S. was also supported by U.S. Department of Energy Grant No. W-7405-ENG-82. We thank N. Papanicolaou and G. Psaltakis for valuable discussions.

APPENDIX

One can find analytically in the limit of $U/B \rightarrow \infty$ the line of instability of the ferromagnetic state towards a phase-separated F-AF state, which has lower energy than both the pure F or the pure AF state.

In the limit of $U/B \rightarrow \infty$, $\delta = 1 - n \rightarrow 0$, the Fermi level for the F state is very close to the upper band edge, where the E versus k can be approximated by

$$E(k) = 2d|V| - |V|a^2k^2, \quad (\text{A1})$$

where d is the dimensionality. From the relations,

$$n = \frac{a^d}{(2\pi)^d} \int d\mathbf{k}, \quad (\text{A2})$$

$$E^{(\text{F})} = \frac{a^d}{(2\pi)^d} \int E(k) d\mathbf{k}, \quad (\text{A3})$$

where the integration is for k within the Fermi "volume" and $E^{(\text{F})}$ is the ferromagnetic energy, we obtain

$$k_{\text{F}a} = (c_d \delta)^{1/d} \quad (\text{A4})$$

and

$$E^{(\text{F})} = -2d|V|\delta + |V|c'_d \delta^{d+2/d}, \quad (\text{A5})$$

where c_d, c'_d are numerical constants which depend on the dimensionality.

The F-AF phase-separated state has an energy versus n curve which is a straight line passing through the $E^{(\text{AF})}$ for $n=1$ and being tangential to the $E^{(\text{F})}$ versus n curve. Hence, its equation is

$$E^{(\text{PS})} = E^{(\text{F})}(n_c) + (n - n_c) \left[\frac{dE^{(\text{F})}}{dn} \right]_{n=n_c}, \quad (\text{A6})$$

where the critical point n_c is determined by the condition

$$E^{(\text{F})}(n_c) + (1 - n_c) \left[\frac{dE^{(\text{F})}}{dn} \right]_{n=n_c} = E^{(\text{AF})}(n=1). \quad (\text{A7})$$

Combining the above equations we find

$$\delta_c = \left[\frac{d}{2c'_d} \frac{|E^{(\text{AF})}(n=1)|}{V} \right]^{d/(2+d)}. \quad (\text{A8})$$

However, for $U/B \rightarrow \infty$ the quantity $E^{(\text{AF})}(n=1)$ is given by (including quantum fluctuations correlations)

$$E^{(\text{AF})}_{(1)} = c''_d \frac{V^2}{U}, \quad (\text{A9})$$

where $c''_d = 4 \ln 2 \approx 2.77, 4.68, 6.582$ for $d = 1, 2, 3$, respectively. Hence,

$$\frac{|V|}{U} = \frac{2c'_d}{dc''_d} \delta_c^{1+(2/d)}. \quad (\text{A10})$$

For $d=1$, $c'_d = \pi^2/3$, and

$$\frac{|V|}{U} = \frac{\pi^2}{6 \ln 2} \delta_c^3 \approx 2.37 \delta_c^3; \quad d=1. \quad (\text{A11})$$

For $d=2$, $c'_d = 2\pi$, and

$$\frac{|V|}{U} = \frac{2\pi}{4.68} \delta_c \approx 1.34 \delta_c^2; \quad d=2. \quad (\text{A12})$$

For $d=3$, $c'_d = (6\pi^2)^{5/3}/10\pi^2$, and

$$\frac{|V|}{U} \approx 0.92 \delta_c^{5/3}; \quad d=3. \quad (\text{A13})$$

*Present address: Department of Chemistry, Rm. 6-224, Massachusetts Institute of Technology, Cambridge, MA 02139.

†Permanent address: Ames Laboratory and Department of Physics, Iowa State University, Ames, IA 50011.

¹M. Marder, N. Papanicolaou, and G. C. Psaltakis, Phys. Rev. B **40**, 6920 (1990); V. J. Emery, S. A. Kirelson, and Q. Lin, Phys. Rev. Lett. **64**, 475 (1990).

²J. Hubbard, Proc. R. Soc. London Ser. A **276**, 236 (1963).

³F. C. Zhang and T. M. Rice, Phys. Rev. B **37**, 3759 (1988).

⁴P. W. Anderson, Science **235**, 1196 (1987), in *Frontiers and Borderlines in Many Particle Physics*, Proceedings of the International School of Physics "Enrico Fermi," Varenna, 1987, edited by R. A. Broglia, Course 104, and J. R. Schrieffer (North-Holland, Amsterdam, 1988), p. 1, and references therein.

- therein.
- ⁵S. R. White, D. J. Scalapino, R. L. Sugar, E. Y. Loh, J. E. Gubernatis, and R. T. Scalettar, *Phys. Rev. B* **40**, 506 (1989); J. E. Hirsch and S. Tang, *Phys. Rev. Lett.* **62**, 591 (1989).
- ⁶S. Sorella, R. Car, S. Baroni, and M. Parrinello, *Europhys. Lett.* **8**, 663 (1989); S. Sorella *et al.*, *Int. J. Mod. Phys.* **3**, 149 (1989); A. Parola *et al. ibid.* **3**, 144 (1989).
- ⁷J. Callaway, D. P. Chen, D. G. Kanhere, and Qiming Li, *Phys. Rev. B* **42**, 465 (1990).
- ⁸A. N. Andriotis, Qiming Li, E. N. Economou, and C. M. Soukoulis, in *Dynamics of Magnetic Fluctuations in High-Temperature Superconductors*, edited by G. Reiter, P. Horsch, and G. C. Psaltakis (Plenum, New York, 1991).
- ⁹E. N. Economou, C. T. White, and R. R. DeMarco, *Phys. Rev. B* **18**, 3946 (1978); C. T. White and E. N. Economou, *ibid.* **18**, 3959 (1978); R. R. DeMarco, E. N. Economou, and C. T. White, *ibid.* **18**, 3968 (1978); E. N. Economou and P. Mihas, *J. Phys. C* **10**, 5017 (1977); E. N. Economou and C. T. White, *Phys. Rev. Lett.* **38**, 289 (1977).
- ¹⁰S. H. Liu, *Phys. Rev. B* **17**, 3629 (1978).
- ¹¹A. N. Andriotis, P. N. Pouloupoulos, and E. N. Economou, *Solid State Commun.* **39**, 1175 (1981).
- ¹²E. N. Economou, *Green's Functions in Quantum Physics* (Springer-Verlag, Heidelberg, 1983).
- ¹³A. N. Andriotis, E. N. Economou, and C. M. Soukoulis (unpublished).
- ¹⁴A. N. Andriotis and J. E. Lowther, *J. Phys. F* **16**, 1189 (1986).
- ¹⁵Y. Nagaoka, *Phys. Rev.* **147**, 392 (1966).
- ¹⁶M. Ogata, M. U. Luchini, S. Sorella, and F. F. Assaad, *Phys. Rev. Lett.* **66**, 2388 (1991).
- ¹⁷H. J. Schulz, *Phys. Rev. Lett.* **64**, 2831 (1990).
- ¹⁸A. Parola and S. Sorella, *Phys. Rev. Lett.* **64**, 1831 (1990).
- ¹⁹M. Inui and P. B. Littlewood, *Phys. Rev. B* **44**, 4415 (1991).